Journal of Catalysis 273 (2010) 39–49

Contents lists available at ScienceDirect

Journal of Catalysis

journal homepage: www.elsevier.com/locate/jcat

Promotional role of H_2O in the selective catalytic reduction of NO with CO over $Ir/WO_3/SiO_2$ catalyst

Masaaki Haneda [a,*], Hideaki Hamada [b]

[a] Ceramics Research Laboratory, Nagoya Institute of Technology, 10-6-29 Asahigaoka, Tajimi, Gifu 507-0071, Japan
[b] Research Center for New Fuels and Vehicle Technology, National Institute of Advanced Industrial Science and Technology (AIST), AIST Tsukuba Central 5, 1-1-1 Higashi, Tsukuba, Ibaraki 305-8565, Japan

ARTICLE INFO

Article history:
Received 2 March 2010
Revised 26 April 2010
Accepted 27 April 2010

Keywords:
Nitrogen monoxide
Selective reduction
Carbon monoxide
Iridium
Tungsten oxide
Water vapor

ABSTRACT

The catalytic activity of $Ir/WO_3/SiO_2$ for the selective reduction of NO with CO in the presence of excess O_2 was significantly increased by the presence of H_2O, whereas NO reduction hardly occurred in the absence of H_2O. Exposure of the reaction gas with H_2O to $Ir/WO_3/SiO_2$ at high temperature led to the stabilization and/or regeneration of reduced Ir sites, as suggested by X-ray diffraction and Raman spectroscopy. Temperature-programmed reduction by H_2 and a combination of scanning transmission electron microscopy and elemental analysis showed the presence of a strong Ir–W oxide interaction. Based on the activity and characterization results, we concluded that the promoting effect of coexisting H_2O is accounted for by the formation of the catalytically active reduced Ir sites, by H_2 produced *in situ* via water gas shift reaction, interacting strongly with W oxide dispersed on SiO_2 via migration of Ir to W oxide or vice versa.

1. Introduction

Catalytic reduction of NO in vehicle exhaust plays an important role in reducing NO_x. Although three-way catalysts for gasoline-fueled vehicles have been commercialized, this cannot be applied to oxygen-rich exhaust emissions such as those from diesel and lean burn engines. In this regard, a great number of studies have been made on the use of hydrocarbons as a reductant for the selective catalytic reduction of NO (HC-SCR) [1–3], since the first reports by Iwamoto et al. [4] and Held et al. [5] following the patents of Volkswagen [6] and Toyota Central R&D Labs [7]. Many kinds of catalysts based on zeolites [8], metal oxides [9], and noble metals [10] have been reported to show activity for HC-SCR. Nevertheless, practical application of HC-SCR has not been realized so far due to insufficient performance in real-life applications. In particular, catalyst deactivation and reaction inhibition by coexisting SO_2 and H_2O are major problems to be solved.

In addition to hydrocarbons, H_2 and CO have recently been proved to act as effective reductants for NO reduction under lean conditions. In 1997, Yokota et al. [11] reported the activity of Pt/mordenite for the selective catalytic reduction of NO with H_2 (H_2-SCR) in the presence of O_2 around 150 °C. They also found that the addition of Mo and Na widens the temperature window. Later, several researchers studied H_2-SCR over Pt- and Pd-based catalysts [12–17]. Although H_2-SCR is a promising approach to the efficient reduction of NO in the presence of O_2 at relatively low temperatures below 200 °C, the production and supply of H_2 is a difficult problem to solve from a practical point of view. On the other hand, CO is a more practical reductant than H_2, because a new type of internal combustion engine developed recently for the reduction of NO_x emission, the so-called homogeneous charge compression ignition (HCCI) engine, emits a relatively high concentration of CO [18], and CO can also be produced easily by engine operation when its amount is insufficient.

Various materials have been examined so far for catalytic performance in the selective catalytic reduction of NO with CO in the presence of O_2 (CO-SCR). To our knowledge, an article by Tauster and Murrell is the first report on the CO-SCR reaction, which takes place over Ir/Al_2O_3 [19]. Ogura et al. [20] found that NO can successfully be reduced to N_2 with CO over an Ir/silicalite catalyst and that the catalytic activity is not influenced by coexisting SO_2. Wang et al. [21] reported that Ir/ZSM-5 was effective for NO reduction with CO under lean conditions. Shimokawabe et al. [22–25] reported that Ir/WO_3 and Ir/ZnO show high activity for NO reduction with CO and that Ir/WO_3 is effective even in the presence of SO_2. Nanba et al. [26,27] found that the $Ir/WO_3–SiO_2$ catalyst shows high activity at a high space velocity (~50,000 h^{-1}). The CO-SCR reaction was also reported to take place catalytically over supported metal oxide catalysts such as Cu/Al_2O_3 [28] and Mn/TiO_2

---

* Corresponding author. Fax: +81 572 27 6812.
E-mail address: haneda.masaaki@nitech.ac.jp (M. Haneda).

0021-9517/$ - see front matter © 2010 Elsevier Inc. All rights reserved.
doi:10.1016/j.jcat.2010.04.021

[29]. Although comparison of the activity of various supported metallic catalysts under the same reaction conditions is very difficult, iridium is a promising catalytically active species for NO reduction with CO.

We have also made extensive studies on CO-SCR over Ir/SiO_2-based catalysts since the first report in 2001 [30]. The most interesting feature we have found is that the coexistence of O_2 and SO_2 is essential for NO reduction to occur over Ir/SiO_2 catalysts [31]. By combining surface science techniques using a single-crystal model catalyst and a real catalyst [32], it was found that the coexisting SO_2 stabilizes the catalytically active reduced Ir site. Furthermore, we have found that the addition of Ba [33], WO_3 [34], Nb_2O_5 [35], and both Ba and WO_3 [36] to Ir/SiO_2 drastically enhances its NO reduction activity. In particular, WO_3 and Nb_2O_5 promoted Ir/SiO_2 are highly active catalysts for NO reduction with CO even in the absence of SO_2. This is quite a favorable characteristic for the treatment of diesel exhaust, because of the ever-decreasing sulfur content in diesel fuels.

In addition to small quantities of SO_2, diesel exhaust invariably has excess H_2O. The influence of H_2O on the HC-SCR reaction has been extensively studied, and for many catalysts the presence of H_2O was found to be detrimental to NO conversion. A few catalysts, on the other hand, show NO conversion enhancement due to the presence of H_2O [37–39]. The promotional effect of H_2O in HC-SCR is well understood and is correlated with the removal of carbonaceous materials deposited on the catalyst surface and also with the suppression of undesirable hydrocarbon oxidation reactions. However, the effect of H_2O on CO-SCR is not well understood from fundamental and practical application points of view. In the present work, we have investigated in detail the effect of coexisting H_2O on the catalytic activity of $Ir/WO_3/SiO_2$, which showed high activity for CO-SCR [34,40]. The role of coexisting H_2O in promoting NO conversion is discussed based on the reaction data as well as catalyst characterizations such as X-ray diffraction (XRD), Raman spectroscopy, temperature-programmed reduction by H_2 (H_2-TPR), transmission electron microscopy (TEM), and high-angle annular dark-field-scanning transmission electron microscopy (HAADF-STEM) with energy dispersed X-ray spectroscopic (EDS) analyses.

2. Experimental

2.1. Catalyst preparation

Ir/SiO_2 was prepared by incipient wetness impregnation. An aqueous solution of $Ir(NO_3)_3$ (Ishifuku Metal Industry Co., Ltd.) was added to SiO_2 (Fuji Silysia Chemicals, Cariact G-10,300 $m^2\ g^{-1}$). The impregnated catalyst precursor was dried at 110 °C overnight and finally calcined at 600 °C for 6 h in air. The Ir loading was set to 0.5 wt.%.

WO_3/SiO_2 as a support was prepared by an impregnation method using an aqueous solution of $(NH_4)_{10}W_{12}O_{41}\cdot 5H_2O$ and citric acid. SiO_2 was added to the solution and water was evaporated; then the solution it was dried at 110 °C overnight and calcined in flowing air at 500 °C for 5 h. The WO_3:SiO_2 weight ratio was 1:9. The resulting WO_3/SiO_2 powder was then impregnated with a solution of $Ir(NO_3)_3$, followed by drying at 110 °C overnight and calcination at 600 °C for 6 h in air. The catalyst after calcination is abbreviated as "fresh". The loadings of Ir were 0.5, 1, and 5 wt.%.

2.2. Activity tests

Catalytic activity was evaluated using a fixed-bed continuous flow reactor. A catalyst sample (0.04 g) was held in a quartz tube (10-mm i.d.) by packing quartz wool at both ends of the catalyst bed. Prior to each reaction, the catalyst was pretreated *in situ* in a flow of helium at 600 °C for 1 h, unless otherwise specified. In some experiments, the catalyst was pretreated in a flow of either 10% H_2/He or 5% O_2/He at 600 °C for 1 h.

The standard reaction gas containing NO (500 ppm), CO (3000 ppm), O_2 (5%), SO_2 (1 ppm), and H_2O (6%) diluted in He as the balance gas was fed through the catalyst bed at a rate of 90 $cm^3\ min^{-1}$ (SV = ca. 75,000 h^{-1}). In some experiments, the concentration of H_2O was changed from 0% to 10%. The effluent gas was analyzed using two online gas chromatographs equipped, respectively, with a Molecular Sieve 5A column (for the analysis of N_2 and CO) and a Porapak Q column (for the analysis of CO_2 and N_2O). The reaction temperature was decreased from 600 to 200 °C in steps of 20–50 °C, and the steady-state catalytic activity was measured at each temperature. N_2 was mainly formed as the NO reduction products. The selectivity to N_2 ($N_2/(N_2 + N_2O)$) was more than 90% in most cases.

2.3. Catalyst characterization

The crystal structure was identified by XRD measurements using Cu Kα radiation at 40 kV and 150 mA (Mac Science M18XHF^{22}). The Raman spectra were measured with a JASCO NRS-3100 dispersive Raman spectrometer. The excitation was by a green laser (wavelength 532 nm) with a power of ~10 mW measured at the analysis spot. H_2-TPR measurements were carried out to estimate the reducibility of catalysts pretreated under different conditions. The TPR profiles were obtained from room temperature to 600 °C in a 30-$cm^3\ min^{-1}$ flow of 10% H_2/Ar at a heating rate of 10 °C min^{-1}. The consumption of H_2 was monitored using a thermal conductivity detector (TCD). TEM and HAADF-STEM with EDS analyses were performed to examine the position of Ir on WO_3/SiO_2 support. TEM and HAADF-STEM images were obtained with a Tecnai G2 F20 (FEI, The Netherlands), operating at an acceleration voltage of 200 kV. The elemental analysis was performed by combining HAADF images with EDS (EDAX Inc.). The collection time of each EDS analysis was set at 100 s.

3. Results

3.1. Catalytic activity

3.1.1. Comparison of activity of Ir/SiO_2 and $Ir/WO_3/SiO_2$

Fig. 1 compares the activity of Ir/SiO_2 and $Ir/WO_3/SiO_2$ for NO reduction with CO in the presence of O_2 and SO_2 either without or with 6% H_2O, where the loading of Ir was 0.5 wt.%. In the absence of H_2O, Ir/SiO_2 showed slightly higher activity than $Ir/WO_3/SiO_2$. However, the activity of both catalysts was quite low. When 6% H_2O was introduced into the reaction gas, not only NO conversion but also CO conversion was enhanced for both catalysts. In particular, significant activity enhancement was observed for $Ir/WO_3/SiO_2$ catalysts, on which maximum NO conversion was increased from 4% to 79% at 280 °C. The presence of H_2O promotes NO reduction by CO over supported Ir catalysts, and this promotion is more pronounced when WO_3 is present in the catalyst. It is also of interest that a different shape of light-off curve was obtained for CO conversion over $Ir/WO_3/SiO_2$ in the presence of H_2O. Namely, a plateau region, where CO conversion was almost constant, was observed in the temperature range 400–280 °C.

Fig. 2 shows the activity of $Ir/WO_3/SiO_2$ with various Ir loadings for NO reduction with CO in the presence of H_2O. Their activity was compared on the basis of the reaction rate normalized by the total Ir content (mol s^{-1} g-Ir^{-1}). It is apparent that the activity normalized by the Ir content was increased with decreasing Ir loading. The maximum activity was obtained for 0.5 wt% $Ir/WO_3/SiO_2$ in

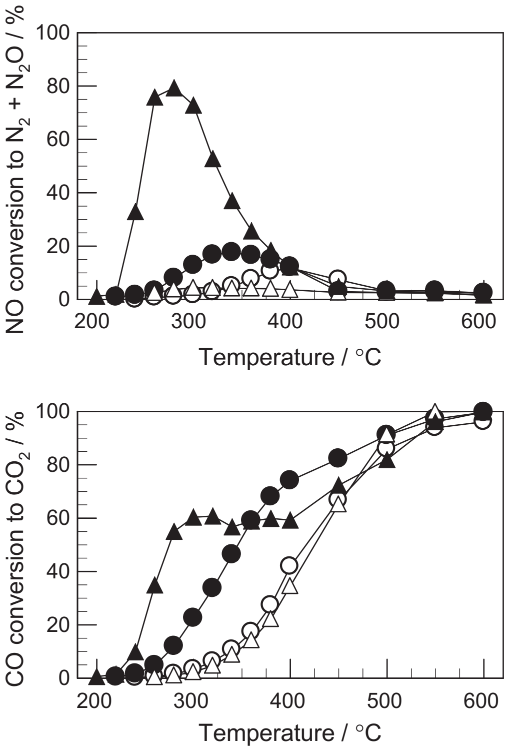

Fig. 1. Comparison of the activity of Ir/SiO_2 (○, ●) and $Ir/WO_3/SiO_2$ (△, ▲) for NO reduction with CO in the presence of O_2 and SO_2 either without (○, △) or with 6% H_2O (●, ▲). Conditions: NO = 500 ppm, CO = 3000 ppm, O_2 = 5%, SO_2 = 1 ppm, H_2O = 0 or 6%, $W/F = 0.0267$ g s cm^{-3}.

the entire temperature range. Since 0.5 wt% $Ir/WO_3/SiO_2$ catalyst showed the best catalytic performance, the rest of this paper deals mainly with this catalyst.

3.1.2. Effect of coexisting H_2O on the activity of $Ir/WO_3/SiO_2$

Fig. 3 shows the activity of $Ir/WO_3/SiO_2$ for NO reduction with CO when H_2O concentration was varied from 0% to 10%. When H_2O was not present in the reaction gas, as described earlier, NO reduction hardly occurred over the entire temperature range, and CO conversion to CO_2 was also low. On the other hand, the presence of 0.75% H_2O caused a significant increase in NO conversion as well as CO conversion. It was also found that the catalytic activity of $Ir/WO_3/SiO_2$ increased with increasing H_2O concentration up to 6%, although the addition of 10% H_2O did not cause a further increase in its activity. It is also noteworthy that the plateau region with constant CO conversion appeared with increasing H_2O concentration.

In the previous reports, the catalytic activity of $Ir/WO_3–SiO_2$ was shown to depend strongly on the catalyst pretreatment conditions [34]. Similarly, the effect of coexisting H_2O on the activity of $Ir/WO_3/SiO_2$ could also be influenced by the pretreatment conditions. As shown in Fig. 4, no activity enhancement by coexisting H_2O was observed for the catalyst pretreated with O_2/He, indicating that the oxidized Ir species is not active component for NO reduction with CO, as already reported [31,34]. On the other hand, a significant enhancement of the activity for NO reduction as well as CO oxidation was achieved when $Ir/WO_3/SiO_2$ was pretreated in He. The NO reduction activity of $Ir/WO_3/SiO_2$ pretreated with H_2/He was also slightly enhanced by coexisting H_2O, whereas CO conversion was decreased, suggesting selectivity improvement for the reaction of NO with CO by coexisting H_2O. In contrast to the catalysts pretreated in He, it is of interest that the reduced $Ir/WO_3/SiO_2$ catalyst showed activity even in the absence of H_2O.

In order to consider the possibility that the promoting effect of coexisting H_2O is related to the change in the catalytically active species, the response of NO conversion to the intermittent feed of H_2O was examined at 300 °C. Here, NO reduction with CO was first monitored in the presence of H_2O from 600 to 300 °C after

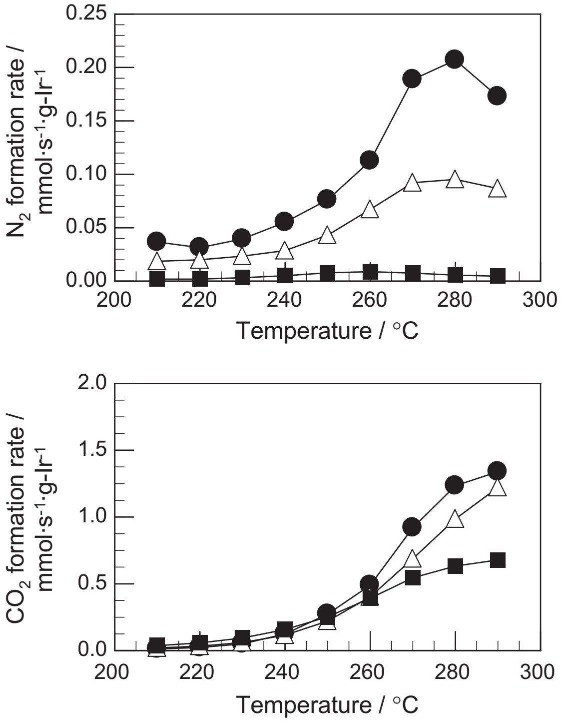

Fig. 2. Activity of $Ir/WO_3/SiO_2$ with various Ir loadings for NO reduction with CO in the presence of H_2O. Conditions: NO = 500 ppm, CO = 3000 ppm, O_2 = 5%, SO_2 = 1 ppm, H_2O = 6%, $W/F = 0.0267$ g s cm^{-3}. (●) Ir = 0.5 wt%, (△) Ir = 1 wt%, (■) Ir = 5 wt%.

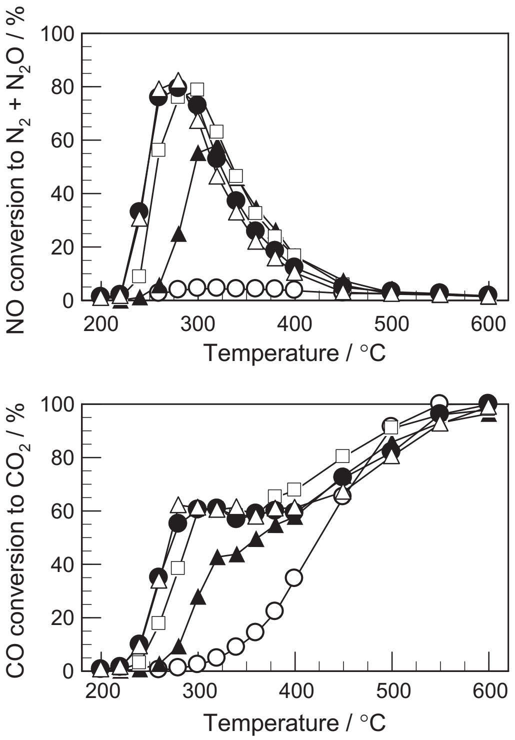

Fig. 3. Effect of H_2O concentration on the activity of $Ir/WO_3/SiO_2$ for NO reduction with CO in the presence of O_2 and SO_2. Conditions: NO = 500 ppm, CO = 3000 ppm, O_2 = 5%, SO_2 = 1 ppm, H_2O = 0–10%, $W/F = 0.0267$ g s cm^{-3}. (○) 0% H_2O, (▲) 0.75% H_2O, (□) 1.5% H_2O, (●) 6% H_2O, (△) 10% H_2O.

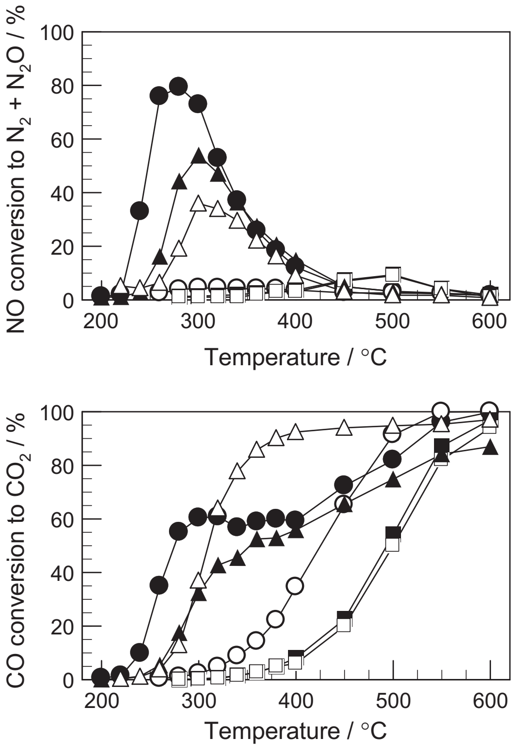

Fig. 4. Effect of pretreatment conditions at 600 °C on the activity of $Ir/WO_3/SiO_2$ for NO reduction with CO in the presence of O_2 and SO_2 without (□, △, ○) or with 6% H_2O (■, ▲, ●). The reaction conditions are the same as for Fig. 1. (□, ■) treated in flowing 5% O_2/He, (△, ▲) treated in flowing 10% H_2/He, (○, ●) treated in flowing He.

the pretreatment of the catalyst with He at 600 °C, and then the removal and introduction of H_2O were carried out at 300 °C. The results are shown in Fig. 5. During the reaction in the presence of H_2O at 300 °C, almost stable activity was obtained. When H_2O was removed from the reaction gas, NO conversion slightly decreased with time but did not reach the value given in Fig. 1 (4%). The subsequent introduction of H_2O did not recover the NO conversion to the initial level. This result suggests that H_2O does not directly participate in the reaction as a reactant. In order to get information on the role of H_2O, the activity of $Ir/WO_3/SiO_2$ for NO reduction with CO in the absence of H_2O was measured from 400 °C, where $Ir/WO_3/SiO_2$ was first pretreated in He at 600 °C and then cooled to 400 °C in flowing He. As shown in Fig. 6, the NO conversions were very similar to those in the presence of H_2O, whereas higher CO conversion was achieved when the reaction was started at 400 °C in the absence of H_2O. This suggests that the catalytic species of $Ir/WO_3/SiO_2$ for NO reduction with CO would be altered by contacting H_2O in the temperature range from 400 to 600 °C.

3.2. Catalyst characterization

The activity of $Ir/WO_3/SiO_2$ for NO reduction with CO was found to be severely affected by coexisting H_2O. To examine the influence of coexisting H_2O on the characteristics of $Ir/WO_3/SiO_2$, various characterizations were performed for $Ir/WO_3/SiO_2$ before and after catalytic tests with or without H_2O.

3.2.1. Structure of $Ir/WO_3/SiO_2$ identified by XRD and Raman spectroscopy

The crystal structure of the catalysts was measured by XRD. As shown in Fig. 7a, distinct XRD peaks due to monoclinic WO_3 (ICDD43-1035) were observed for fresh $Ir/WO_3/SiO_2$ sample. No peaks assignable to Ir species were detected because of small crystallites arguably due to very low Ir loading (0.5 wt.%). After He treatment at 600 °C (Fig. 7b), a decrease in the peak intensity was observed, suggesting the partial reduction of tungsten oxide. Fig. 7c and d shows the XRD patterns of $Ir/WO_3/SiO_2$ after catalytic tests with or without H_2O. It is apparent that no significant difference in the XRD patterns was observed, irrespective of the history of $Ir/WO_3/SiO_2$ samples, suggesting that the crystal structure of $Ir/WO_3/SiO_2$ is stable even after use in the reaction. On the other hand, the peak intensity of XRD peaks after use in the reaction with H_2O was significantly low (Fig. 7d). This XRD pattern is very similar to that obtained after He treatment (Fig. 7b). The partial reduction of tungsten oxide is presumed to occur during the reaction in the presence of H_2O.

Since Raman spectroscopy is a more sensitive technique for identifying changes in M—O bond arrangement, the Raman spectra of $Ir/WO_3/SiO_2$ before and after use in the reaction with or without H_2O were analyzed (Fig. 8). On the fresh $Ir/WO_3/SiO_2$ sample, six distinct Raman bands centered at 970, 800, 712, 549, 325, and 260 cm^{-1} were detected (Fig. 8a). According to the literature

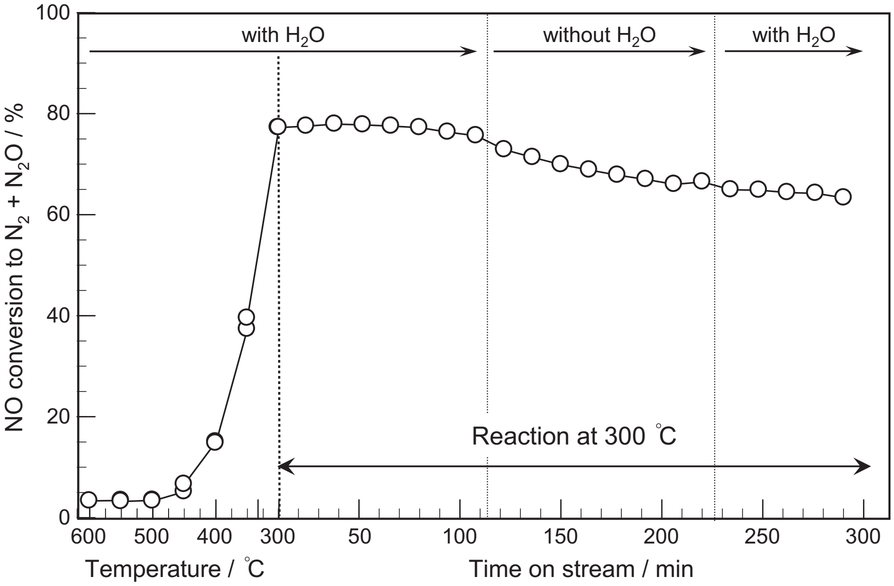

Fig. 5. Response of NO conversion to N_2 + N_2O to intermittent feed of 6% H_2O over $Ir/WO_3/SiO_2$ at 300 °C. The reaction conditions are the same as for Fig. 1.

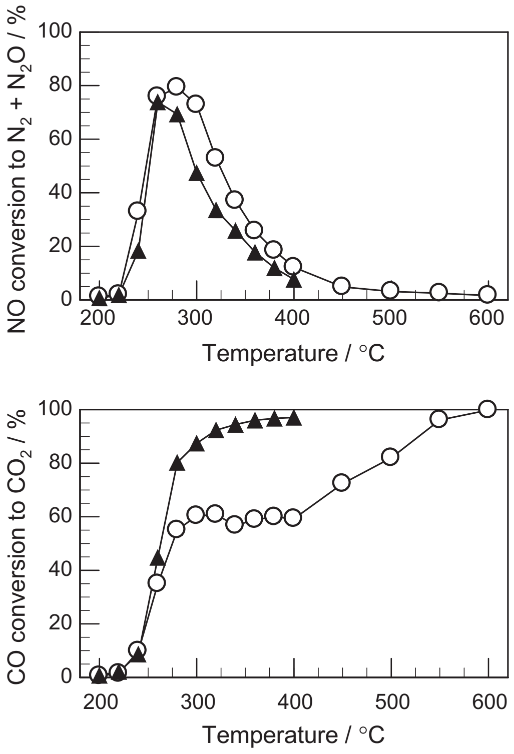

Fig. 6. Comparison of the activity of $Ir/WO_3/SiO_2$ for NO reduction with CO performed in the presence of H_2O from 600 °C (○) and in the absence of H_2O from 400 °C (▲). Conditions are the same as for Fig. 1.

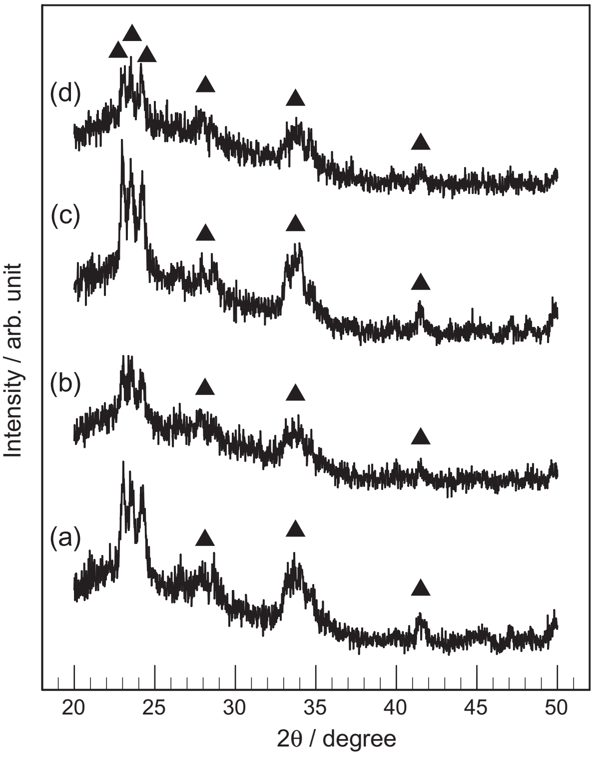

Fig. 7. XRD patterns of $Ir/WO_3/SiO_2$: (a) fresh, (b) after He treatment at 600 °C, (c) after use in the reaction without H_2O, and (d) with H_2O, (▲) for WO_3.

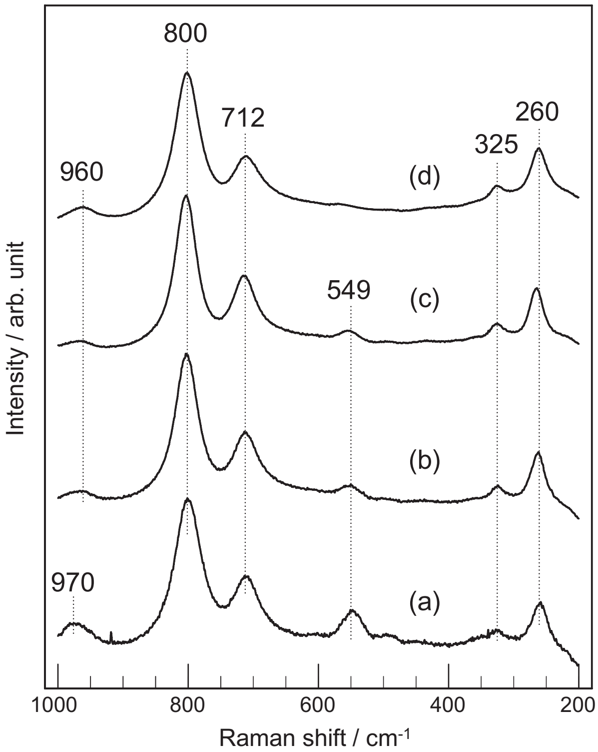

Fig. 8. Raman spectra of $Ir/WO_3/SiO_2$: (a) fresh, (b) after He treatment at 600 °C, (c) after use in the reaction without H_2O, and (d) with H_2O.

[41–44], monoclinic WO_3 gives rise to Raman bands at 808, 717, 317, and 273 cm^{-1}, and IrO_2 shows Raman bands at 718 and 544 cm^{-1}. Therefore, the Raman bands detected for the fresh $Ir/WO_3/SiO_2$ sample at 800 and 712 cm^{-1} can be assigned to the O—W—O stretching modes of monoclinic WO_3, and the bands at 325 and 260 cm^{-1} are the corresponding bending modes. This is in accordance with the results of XRD (Fig. 7). The Raman band at 549 cm^{-1} can be assigned to IrO_2, whereas the other Raman band, which would be detected at 718 cm^{-1}, is overlapped with the band due to the O—W—O stretching modes of monoclinic WO_3. Iridium was found to be present as IrO_2 in the catalyst, although the identification of Ir species was difficult from the XRD data.

The Raman band at around 970 cm^{-1} can be assigned to the stretching mode of the terminal W═O bond, a characteristic band of hydrated WO_3 [41,42]. The frequency of the Raman band due to the terminal W═O bond depends on the hydration level of WO_3, i.e., $WO_3 \cdot 1/3H_2O$, $WO_3 \cdot H_2O$, and $WO_3 \cdot 2H_2O$, and shifts to higher position with the hydration level [41]. As can be seen in Fig. 8, a shift of the Raman band due to the terminal W═O bond to lower frequency was observed after He treatment and after use in the reaction. Although the determination of the hydration level of WO_3 in each sample is difficult, the hydration level of WO_3 seems to be decreased by sample treatment.

Obviously, the intensity of the Raman band at 549 cm^{-1} assignable to IrO_2 was decreased after He treatment at 600 °C (Fig. 8b), suggesting that part of IrO_2 is reduced. No significant change in the intensity of the band at 549 cm^{-1} was observed for $Ir/WO_3/SiO_2$ after use in the reaction without H_2O (Fig. 8c). When the sample was used in the reaction with H_2O, on the other hand, the Raman band due to IrO_2 almost completely disappeared (Fig. 8d). This indicates that the reduction of IrO_2 is accelerated in the presence of H_2O.

3.2.2. Reduction behavior of $Ir/WO_3/SiO_2$ by H_2-TPR

Fig. 9 shows TPR profiles of $Ir/WO_3/SiO_2$, as well as Ir/SiO_2 and WO_3/SiO_2 as reference samples. Ir/SiO_2 (profile a) and WO_3/SiO_2 (profile b) oxidized in flowing 20% O_2/N_2 at 600 °C before

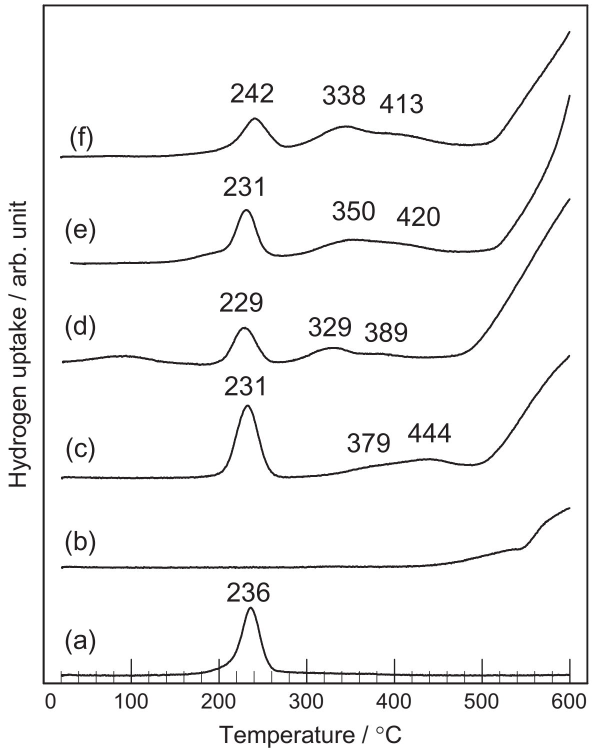

Fig. 9. TPR profiles of (a) Ir/SiO_2, (b) WO_3/SiO_2, (c) $Ir/WO_3/SiO_2$ oxidized at 600 °C, (d) $Ir/WO_3/SiO_2$ after He treatment at 600 °C, (e) $Ir/WO_3/SiO_2$ after use in the reaction without H_2O, and (f) with H_2O.

measurement gave peaks at 236 °C and above 450 °C, respectively. These peaks are due to the reduction of IrO_2 and WO_3. In the TPR profile of $Ir/WO_3/SiO_2$ oxidized at 600 °C (profile c), broad H_2 consumption peaks were detected at 379 and 444 °C in addition to the two peaks. These peaks would be ascribed to the reduction of oxygen present at the Ir–WO_3 interface, because no such peaks were observed for Ir/SiO_2 and WO_3/SiO_2.

A significant decrease in the area of the low-temperature peak and a shift of the middle-temperature peaks to lower temperatures (329, 389 °C) were observed for $Ir/WO_3/SiO_2$ treated with He (profile d). As given in profile e, an increase in the area of the low-temperature peak and a shift of the middle-temperature peaks to high temperature (350, 420 °C) were observed for $Ir/WO_3/SiO_2$ after use in the reaction without H_2O, where the sample was not pretreated before measurement. The shape of this TPR profile is similar to that for $Ir/WO_3/SiO_2$ oxidized at 600 °C (profile c), compared with that for $Ir/WO_3/SiO_2$ treated with He. The surface of $Ir/WO_3/SiO_2$ seems to be oxidized under the reaction conditions in the absence of H_2O. On the other hand, $Ir/WO_3/SiO_2$ after use in the presence of H_2O (profile f) gave a TPR profile with a different feature from that for the sample after use in the reaction without H_2O. Namely, a significant decrease in the area of the low-temperature peak and a shift of the middle-temperature peaks to lower temperature (338, 413 °C) were observed. In addition, the low-temperature peak clearly shifted to higher temperature (231 → 242 °C). These results lead us to the conclusion that the state of Ir species was altered by coexisting H_2O.

4. Discussion

4.1. Role of coexisting H_2O

The catalytic performance of $Ir/WO_3/SiO_2$ for the selective reduction of NO with CO in the presence of excess O_2 was significantly influenced by coexisting H_2O. NO reduction hardly occurred over the entire temperature range under the reaction conditions in the absence of H_2O, whereas the catalytic activity of $Ir/WO_3/SiO_2$ increased with increasing H_2O concentration up to 6% (Fig. 3). This clearly suggests that the presence of coexisting H_2O is essential for NO reduction to occur. It was also found that the promoting effect of coexisting H_2O is strongly dependent on the pretreatment condition of $Ir/WO_3/SiO_2$ catalyst (Fig. 4). $Ir/WO_3/SiO_2$ oxidized at 600 °C before the reaction showed little activity irrespective of coexisting H_2O. However, significant enhancement of the activity was achieved on the catalyst treated in He at 600 °C. On the other hand, when the reaction in the absence of H_2O was started from 400 °C after pretreatment in He at 600 °C, the NO conversions were very similar to those for the reaction started from 600 °C in the presence of H_2O (Fig. 6). This finding suggests that coexisting H_2O does not directly participate in the reaction as a reactant.

The response of NO conversion to the intermittent feed of H_2O also gave us the same suggestion. If H_2O directly participates in the reaction as a reactant, NO conversion should instantaneously reverse, depending on the presence or absence of H_2O. However, as shown in Fig. 5, NO conversion decreased slightly with time when H_2O was removed from the reaction gas, and the subsequent introduction of H_2O did not restore the NO conversion to the initial level. Therefore, the promoting effect of coexisting H_2O would be related to the change in the catalytically active Ir species in the temperature range 400–600 °C.

As already reported [31], Ir species in the reduced state act as the reaction site for NO reduction with CO. Taking into account the fact that $Ir/WO_3/SiO_2$ pretreated in He at 600 °C catalyzes effectively NO reduction with CO in the absence of H_2O, when the reaction was started at 400 °C (Fig. 6), the reduced Ir species is presumed to be formed by He treatment at 600 °C. In fact, the intensity of the Raman band at 549 cm^{-1} due to IrO_2 clearly decreased after He pretreatment (Fig. 8b). In addition, a significant decrease in the area of the H_2 consumption peak due to the reduction of IrO_2 (229 °C) in the H_2-TPR profile was observed after He pretreatment at 600 °C (Fig. 9d), suggesting slight reduction of Ir species. On the other hand, the reduced Ir species formed by He treatment at 600 °C can be expected to be oxidized during the reaction because excess O_2 (5%) is present in the reaction gas. The deactivation observed when the reaction was carried out in the absence of H_2O at 300 °C (Fig. 5) is presumed to be due to the oxidation of Ir species. The oxidation of Ir species would be more prominent at temperatures above 400 °C in the absence of H_2O. Consequently, coexisting H_2O is considered to prevent catalyst deactivation caused by oxidation of the catalytically active Ir sites. Since the Raman band due to IrO_2 observed at 549 cm^{-1} for $Ir/WO_3/SiO_2$ after He treatment almost completely disappeared after the reaction in the presence of H_2O (Fig. 8d), coexisting H_2O would also participate in the regeneration of the catalytically active reduced Ir sites.

Thus, a question arises: how can the catalytically active Ir sites be stabilized and/or regenerated during the reaction in the presence of H_2O? Since the reaction gas employed in this study contains CO and H_2O, the formation of H_2 by the water gas shift (WGS) reaction can be expected. Supported Ir catalysts have been reported to show activity for WGS reaction [45,46]. In fact, as shown in Fig. 10, a certain amount of CO_2 is formed when a gas mixture of CO and H_2O is exposed to $Ir/WO_3/SiO_2$ at temperatures above 400 °C. This result suggests that the WGS reaction is taking place on the $Ir/WO_3/SiO_2$ catalyst, although H_2 was not detected because of its consumption in the reduction of Ir oxide. To examine the effect of H_2, the activity of $Ir/WO_3/SiO_2$ for NO reduction with CO in the absence of H_2O and in the presence of 1000 ppm H_2 was monitored. As shown in Fig. 11, the activity of $Ir/WO_3/SiO_2$ was clearly increased by addition of H_2. However, its activity was lower than that obtained in the presence of H_2O. This is probably

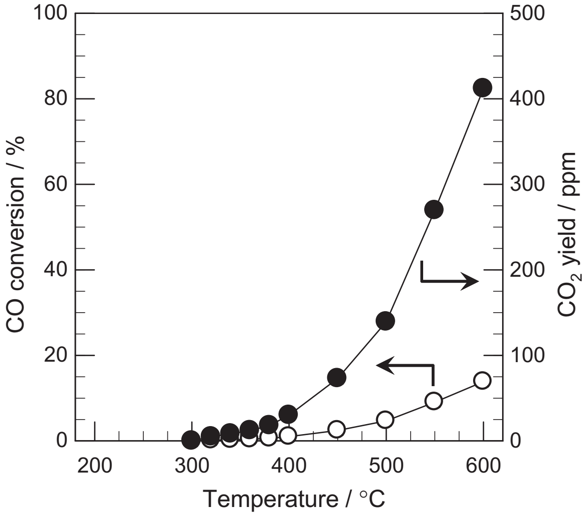

Fig. 10. Activity of $Ir/WO_3/SiO_2$ pretreated in He at 600 °C for water gas shift (WGS) reaction. Conditions: CO = 3000 ppm, H_2O = 6%, $W/F = 0.0267$ g s cm^{-3}. (○) CO conversion, (●) CO_2 yield.

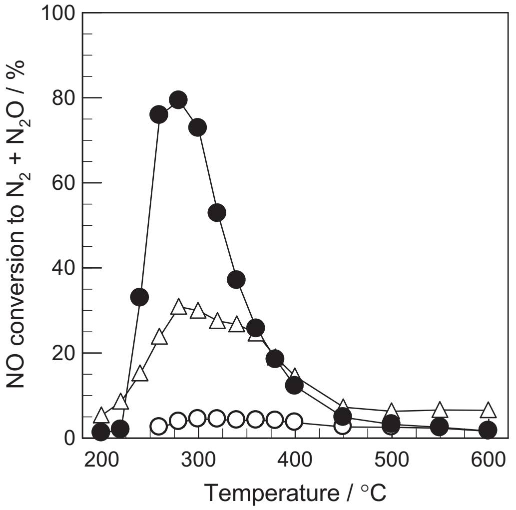

Fig. 11. Effect of H_2 addition on the activity of $Ir/WO_3/SiO_2$ for NO reduction with CO in the absence of H_2O. Conditions: NO = 500 ppm, CO = 3000 ppm, O_2 = 5%, SO_2 = 1 ppm, H_2O = 0% or 6%, H_2 = 0 or 1000 ppm, $W/F = 0.0267$ g s cm^{-3}. (○) H_2O = 0%, H_2 = 0 ppm, (●) H_2O = 6%, H_2 = 0 ppm, (△) H_2O = 0%, H_2 = 1000 ppm.

because most of the added H_2 is consumed by the reaction with O_2. H_2 produced *in situ* via the WGS reaction would be efficiently used to produce the reduced Ir species. Erdőhelyi et al. [45] reported that the WGS reaction on supported Ir catalysts proceeds depending on the 0.26 order of H_2O, suggesting that H_2 formation increases with H_2O concentration. The result that the catalytic activity of $Ir/WO_3/SiO_2$ increases with increasing H_2O concentration up to 6% (Fig. 2) is probably due to an increase in the amount of H_2 produced *in situ* via the WGS reaction. We can conclude that coexisting H_2O plays an essential role in NO reduction over $Ir/WO_3/SiO_2$ catalyst through the stabilization and/or regeneration of catalytically active Ir sites in the reduced state by H_2 produced *in situ* via the WGS reaction.

4.2. Formation of Ir–WO_3 interaction by coexisting H_2O

Since coexisting H_2O contributes to the stabilization and/or regeneration of catalytically active reduced Ir species, as discussed earlier, its promoting effect should be observed generally for supported Ir catalysts. In fact, as shown in Fig. 1, the activity of Ir/SiO_2 and $Ir/WO_3/SiO_2$ was enhanced by the addition of H_2O to the reaction gas. However, more significant activity enhancement was achieved for the $Ir/WO_3/SiO_2$ catalyst, suggesting the participation of WO_3 as the catalytically active sites. We have recently reported that the active sites of $Ir/WO_3/SiO_2$ for NO reduction with CO are Ir–WO_x ($x = 2.92{-}3$) species in which Ir metal interacts strongly with W oxide and Ir–WO_x species that promote NO dissociation, which is the first step for NO reduction with CO [34]. This means that the interaction between reduced Ir species and W oxide is necessary for the NO reduction activity. To clarify the importance of Ir–WO_x species, turnover frequency (TOF) for NO reduction to N_2, expressed as moles of NO reduced to N_2 per mole of surface Ir atoms per second over 0.5 wt% Ir/SiO_2 and 0.5 wt% $Ir/WO_3/SiO_2$, was calculated. Since no CO chemisorption on $Ir/WO_3/SiO_2$ was observed [40], number of surface Ir atoms was estimated from the crystallite size of IrO_2 evaluated from Raman bands. On the other hand, Ir dispersion in Ir/SiO_2 was found to be 0.10 from CO chemisorption [40]. In Table 1 are summarized the number of Ir atoms exposed on the surface calculated here. As shown in Fig. 12, a quite high TOF was obtained for $Ir/WO_3/SiO_2$, suggesting that Ir–WO_x species created by the interaction of reduced Ir species and W oxide are highly active species for NO reduction compared with reduced Ir species.

The participation of reduced Ir species and W oxide as the catalytically active sites is also supported by the fact that $Ir/WO_3/SiO_2$ pretreated with He at 600 °C show higher NO reduction activity than that pretreated with H_2/He (Fig. 4). Namely, partially reduced Ir species and W oxide species are present in the $Ir/WO_3/SiO_2$ pretreated with He at 600 °C, as described in the previous section, resulting in the formation of Ir–W oxide interaction. On the other hand, fully reduced W species after H_2 treatment are not activated to oxide species during the reaction, suggesting no formation of Ir–W oxide interaction. These results lead us to the consideration that the formation behavior of Ir–W oxide interaction is different depending on the history of $Ir/WO_3/SiO_2$.

Table 1
Crystallite size of IrO_2, Ir dispersion, and the number of Ir atoms exposed on the surface calculated.

	Crystallite size of IrO_2 estimated from Raman band (nm)	Ir dispersion estimated from CO chemisorption (Ir/CO)	Number of Ir atoms exposed on the surface (atoms g-cat^{-1})
Ir/SiO_2	Not available	0.10	1.57×10^{18}
$Ir/WO_3/SiO_2$	4	Not available	5.71×10^{18}

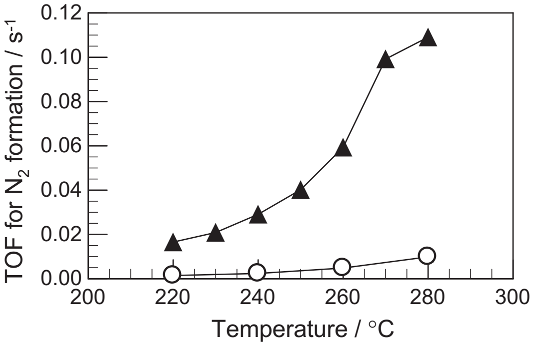

Fig. 12. Turnover frequency for NO reduction to N_2 over Ir/SiO_2 (○) and $Ir/WO_3/SiO_2$ (▲). The reaction conditions are the same as for Fig. 2.

Table 2
Summary of H_2-TPR measurements.

	Peak temperature (°C)		Amount of H_2 consumption (μmol-H_2 g-cat^{-1})	
	Low-temperature peak	Middle-temperature peaks	Low-temperature peak	Middle-temperature peaks
Ir/SiO_2	236	Not detected	31.5	Not detected
WO_3/SiO_2	Not detected	Not detected	Not detected	Not detected
$Ir/WO_3/SiO_2$ (fresh)	232	379,444	31.8	33.5
$Ir/WO_3/SiO_2$ (He treatment)	229	329,389	17.8	46.0
$Ir/WO_3/SiO_2$ (after use: without H_2O)	231	350,420	29.7	53.5
$Ir/WO_3/SiO_2$ (after use: with H_2O)	242	338,413	15.8	63.4

The presence of Ir–W oxide interaction is confirmed by H_2-TPR profiles of $Ir/WO_3/SiO_2$. As shown in Fig. 9, $Ir/WO_3/SiO_2$, irrespective of its history, gave a sharp H_2 consumption peak at around 230 °C and broad ones at 330–450 °C. The former peak is due to the reduction of IrO_2 to Ir metal from the comparison with TPR profile of Ir/SiO_2 (Fig. 9a). On the other hand, the latter peaks would be ascribed to the reduction of oxygen present at the Ir–WO_3 interface, because no such peaks were observed for Ir/SiO_2 and WO_3/SiO_2 (Fig. 9b), suggesting the presence of Ir–W oxide interaction in the $Ir/WO_3/SiO_2$ catalysts. However, the strength of Ir–W oxide interaction seems to be different depending on the history of $Ir/WO_3/SiO_2$. When $Ir/WO_3/SiO_2$ was employed for the reaction in the presence of H_2O, a shift of the low-temperature peak to high temperature (242 °C) and of the middle-temperature peaks to lower temperature (338 and 413 °C) was clearly observed (Fig. 9f). On the other hand, no shift of the low-temperature peak and a slight shift of the middle-temperature peaks to lower temperature were observed in the TPR profile for the $Ir/WO_3/SiO_2$ sample after use in the reaction without H_2O (Fig. 9e). In addition, as summarized by the quantitative data of H_2-TPR measurements in Table 2, the amount of H_2 consumption for the middle-temperature peaks, which are due to the reduction of oxygen present at the Ir–WO_3 interface, was clearly increased after use in the reaction with H_2O. These findings suggest that a strong interaction between Ir and W oxide is created during the reaction in the presence of H_2O.

In order to clarify the difference in the Ir–W oxide interaction for $Ir/WO_3/SiO_2$ after use in the reaction without and with H_2O, the measurement of STEM/HAADF images as well as that of ele-

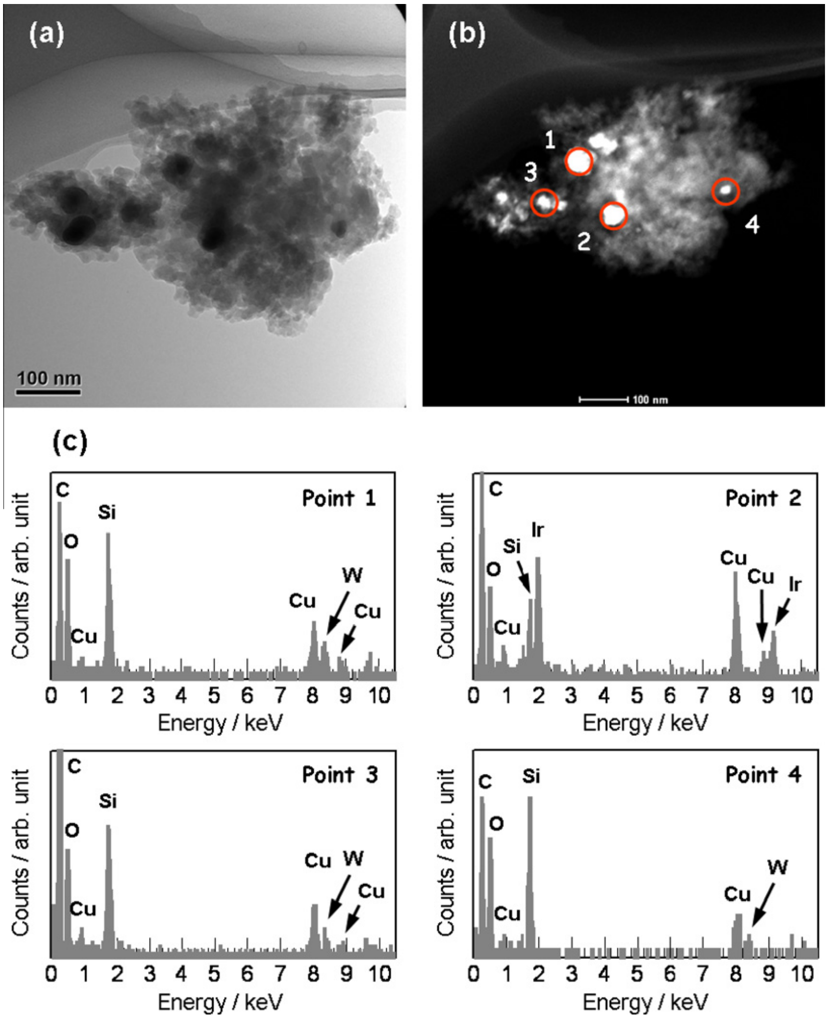

Fig. 13. (a) TEM image, (b) STEM/HAADF image, and (c) EDS spectra of fresh $Ir/WO_3/SiO_2$.

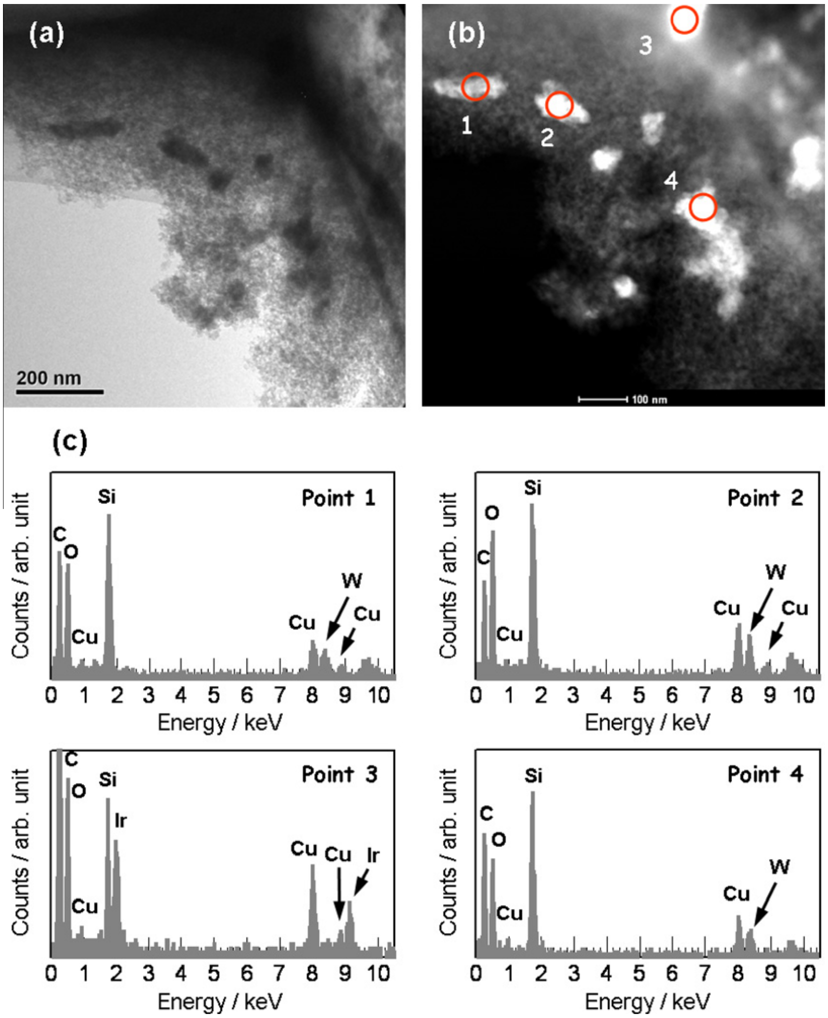

Fig. 14. (a) TEM image, (b) STEM/HAADF image, and (c) EDS spectra of $Ir/WO_3/SiO_2$ after use in the reaction without H_2O.

ment distribution by EDX was performed. Figs. 13–15 show TEM and HAADF images and EDS spectra acquired on $Ir/WO_3/SiO_2$ at various points. For the fresh $Ir/WO_3/SiO_2$ sample (Fig. 13), TEM and HAADF images showed the presence of large particles with a size of 20–70 nm dispersed on SiO_2 support. From the EDS spectra measured for these particles, Ir and W oxide particles were found to be present separately (Fig. 13c). The Si and W signals were observed at points 1, 3, and 4, whereas the Si and Ir signals were detected at point 2. It can be assumed that Ir particles do not directly interact with W oxide particles, although Ir and W oxide are present on the surface of the SiO_2 support. When the $Ir/WO_3/SiO_2$ catalyst was employed for the reaction in the absence of H_2O (Fig. 14), similar morphology and element distribution in the particles was observed. Namely, a separate dispersion of WO_3 (points 1, 2, and 4) and Ir particles (point 3) on SiO_2 support was revealed from EDS spectra (Fig. 14c). This result suggests that, in accordance with the results of H_2-TPR, strong Ir–W oxide interaction is not created during the reaction in the absence of H_2O. The H_2 consumption peaks detected at 350 and 420 °C for this sample (Fig. 9e) would be ascribed to the reduction of W oxide by hydrogen spilled over and migrated from Ir particles.

On the other hand, distribution of Ir and W species in the particles was drastically changed after the reaction in the presence of H_2O (Fig. 15). As can be seen in Fig. 15c, some particles dispersed on SiO_2 support consisted of only W oxide (points 2 and 3). Interestingly, the presence of particles including both Ir and W species was also found (points 1 and 4), indicating the creation of strong Ir–W oxide interaction during the reaction in the presence of H_2O. Nanba et al. [27] reported that the active form in $Ir/WO_3–SiO_2$ catalyst for NO reduction with CO is very fine Ir/WO_3 particles dispersed on SiO_2, and fine Ir/WO_3 particles are formed by sequential treatment involving calcination in the presence of O_2 and H_2O followed by reduction and then reoxidation under mild conditions. On the other hand, the remarkable feature of the present study, which should be pointed out, is that the catalytically active Ir sites in the reduced state interacting strongly with W oxide (Ir–WO_x species) can be created during the reaction in the presence of H_2O without sequential treatment. We can conclude that the promoting effect of coexisting H_2O is ascribable to the formation of the catalytically active Ir–WO_x species dispersed on SiO_2 via migration of Ir to W oxide or vice versa.

5. Conclusions

The activity of supported Ir catalysts, Ir/SiO_2 and $Ir/WO_3/SiO_2$, for the selective reduction of NO with CO in the presence of O_2 was strongly dependent on the concentration of coexisting H_2O in the reaction gas. Supported Ir catalysts did not show activity for NO reduction with CO in the absence of H_2O, whereas their activity was significantly increased by the presence of coexisting H_2O. More significant enhancement of NO reduction activity by coexisting H_2O was achieved on $Ir/WO_3/SiO_2$. On the other hand, when the reaction was carried out starting at 400 °C in the absence

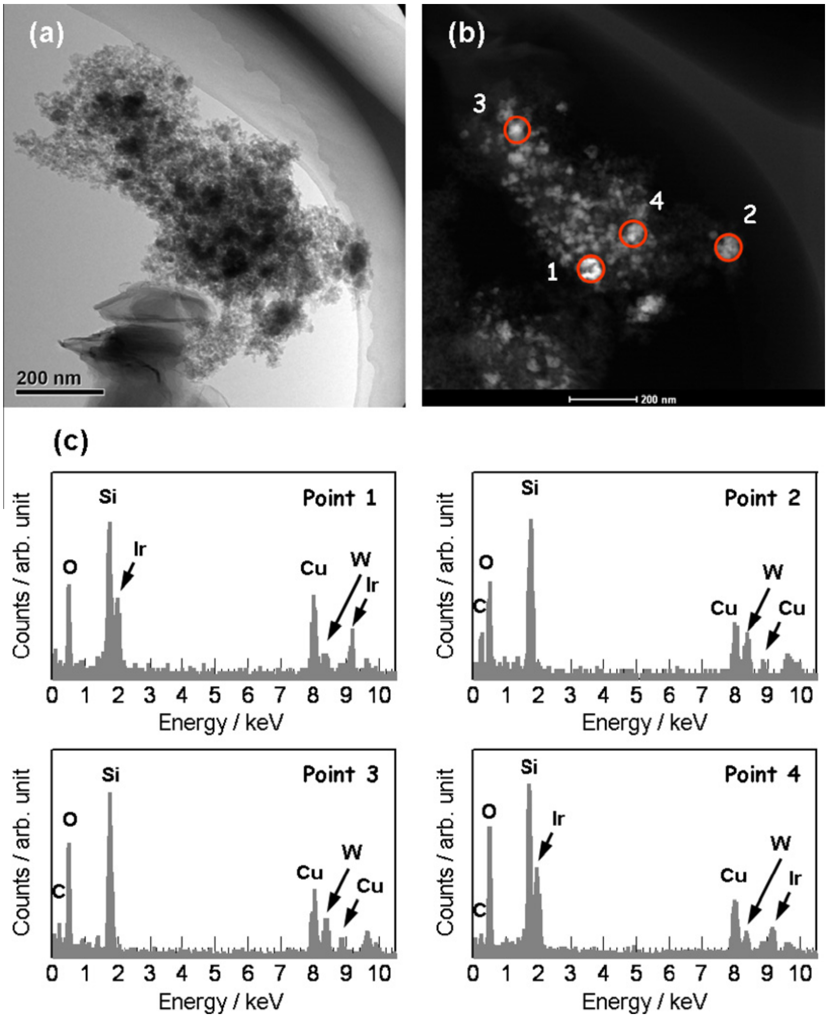

Fig. 15. (a) TEM image, (b) STEM/HAADF image, and (c) EDS spectra of $Ir/WO_3/SiO_2$ after use in the reaction with H_2O.

of H_2O, the NO conversions on $Ir/WO_3/SiO_2$ were very similar to those in the presence of H_2O. In addition, reversible change in the NO conversion to the intermittent feed of H_2O was not observed. From these results, we assumed that coexisting H_2O does not directly participate in the reaction as a reactant.

Structural characterizations by XRD and Raman spectroscopy suggested that the reduced Ir sites formed by He treatment at 600 °C are stabilized and/or regenerated when exposed to high temperature in the presence of H_2O. The catalytically active reduced Ir sites were considered to be stabilized and/or regenerated by the reaction with H_2 produced *in situ* via the WGS reaction. H_2-TPR measurements indicated that the strong Ir–W oxide interaction is created during the reaction in the presence of H_2O. The creation of the strong Ir–W oxide interaction was also visually confirmed by the measurement of STEM/HAADF images as well as that of element distribution by EDX. We concluded that the promoting effect of coexisting H_2O is ascribable to the formation of catalytically active Ir sites in the reduced state, which is formed by H_2 produced *in situ* via the WGS reaction, interacting strongly with W oxide (Ir–WO_x species) dispersed on SiO_2 via migration of Ir to W oxide or vice versa.

Acknowledgments

We express our sincere thanks to Professor Noriyoshi Kakuta and Hironobu Ohkita of Toyohashi University of Technology for their assistance in Raman measurements. We are grateful to Takeyuki Uchida for TEM and HAADF-STEM with EDS analyses supported by the Electron Microscopic Measurement Support Project of AIST, Japan.

References

[1] R. Burch, J.P. Breen, F.C. Meunier, Appl. Catal. B 39 (2002) 283.
[2] R. Burch, Catal. Rev. 46 (2004) 271.
[3] Z. Liu, S.I. Woo, Catal. Rev. 48 (2006) 43.
[4] M. Iwamoto, H. Yahiro, Y. Yu-u, S. Shundo, N. Mizuno, Appl. Catal. 69 (1991) L15.
[5] W. Held, A. König, T. Richter, L. Puppe, SAE Paper 900496, 1990.
[6] W. Held, A. König, Ger. Offen. DE 3642018 (Volkswagen), 1987.
[7] Y. Fujitani, H. Muraki, S. Kondoh, M. Fukui, Ger. Offen. DE 3735151 (Toyota Central R&D Labs.), 1988.
[8] M. Iwamoto, H. Yahiro, Catal. Today 22 (1994) 5.
[9] H. Hamada, Catal. Today 22 (1994) 21.
[10] R. Burch, Catal. Today 26 (1995) 185.
[11] K. Yokota, M. Fukui, T. Tanaka, Appl. Surf. Sci. 121 (/122) (1997) 273.
[12] A. Ueda, T. Nakao, N. Azuma, T. Kobayashi, Catal. Today 45 (1998) 135.
[13] R. Burch, A.A. Shestov, J.A. Sullivan, J. Catal. 188 (1999) 69.
[14] M. Machida, S. Ikeda, D. Kurogi, T. Kijima, Appl. Catal. B 35 (2001) 107.
[15] N. Macloed, R.M. Rambert, Chem. Commun. (2003) 1300.
[16] T. Nanba, C. Kohno, S. Masukawa, J. Uchisawa, N. Nakayama, A. Obuchi, Appl. Catal. B 46 (2003) 353.
[17] M. Itoh, M. Saito, M. Takehara, K. Motoki, J. Iwamoto, K. Machida, J. Mol. Catal. A 304 (2009) 159.
[18] D. Jun, K. Ishi, N. Iida, JSME Int. J. Ser. B 46 (2003) 60.
[19] S.J. Tauster, L.L. Murrell, J. Catal. 41 (1976) 192.
[20] M. Ogura, A. Kawamura, M. Matsukata, E. Kikuchi, Chem. Lett. 29 (2000) 146.
[21] A. Wang, L. Ma, Y. Cong, T. Zhang, D. Liang, Appl. Catal. B 40 (2003) 319.

[22] M. Shimokawabe, N. Umeda, Chem. Lett. 33 (2004) 534.
[23] M. Shimokawabe, M. Niitsu, H. Inomata, N. Iwasa, M. Arai, Chem. Lett. 34 (2005) 1426.
[24] H. Inomata, M. Shimokawabe, M. Arai, Appl. Catal. A 332 (2007) 146.
[25] H. Inomata, M. Shimokawabe, A. Kuwana, M. Arai, Appl. Catal. B 84 (2008) 783.
[26] T. Nanba, S. Shinohara, J. Uchisawa, S. Masukawa, A. Ohi, A. Obuchi, Chem. Lett. 35 (2006) 450.
[27] T. Nanba, S. Shinohara, S. Masukawa, J. Uchisawa, A. Ohi, A. Obuchi, Appl. Catal. B 84 (2008) 420.
[28] T. Yamamoto, T. Tanaka, R. Kuma, S. Suzuki, F. Amano, Y. Shimooka, Y. Kohno, T. Funabiki, S. Yoshida, Phys. Chem. Chem. Phys. 4 (2002) 2449.
[29] P.M. Sreekanth, P.G. Smirniotis, Catal. Lett. 122 (2008) 37.
[30] T. Yoshinari, K. Sato, M. Haneda, Y. Kintaichi, H. Hamada, Catal. Commun. 2 (2001) 155.
[31] M. Haneda, Pusparatu, Y. Kintaichi, I. Nakamura, M. Sasaki, T. Fujitani, H. Hamada, J. Catal. 229 (2005) 197.
[32] T. Fujitani, I. Nakamura, Y. Kobayashi, A. Takahashi, M. Haneda, H. Hamada, Surf. Sci. 601 (2007) 1615.
[33] M. Haneda, H. Kudo, Y. Nagao, T. Fujitani, H. Hamada, Catal. Commun. 7 (2006) 423.
[34] A. Takahashi, I. Nakamura, M. Haneda, T. Fujitani, H. Hamada, Catal. Lett. 112 (2006) 133.
[35] T. Tamai, M. Haneda, T. Fujitani, H. Hamada, Catal. Commun. 8 (2007) 885.
[36] A. Takahashi, T. Fujitani, I. Nakamura, Y. Katsuta, M. Haneda, H. Hamada, Chem. Lett. 35 (2006) 420.
[37] Y. Hirao, C. Yokoyama, M. Misono, J. Chem. Soc. Chem. Commun. (1996) 597.
[38] M. Haneda, Y. Kintaichi, H. Hamada, Appl. Catal. B 20 (1999) 289.
[39] A. Shichi, A. Satsuma, T. Hattori, Chem. Lett. 30 (2001) 44.
[40] M. Haneda, N. Aoki, K. Arimitsu, H. Hamada, Bull. Chem. Soc. Jpn. 82 (2009) 1023.
[41] M.F. Daniel, B. Desbat, J.C. Lassegues, B. Gerand, M. Figlarz, J. Solid State Chem. 67 (1987) 235.
[42] H. Habazaki, Y. Hayashi, H. Konno, Electrochim. Acta 47 (2002) 4181.
[43] S.C. Chan, S.C. Fung, J.H. Sinfelt, J. Catal. 113 (1988) 164.
[44] S. Musić, S. Popović, M. Maljković, Ž. Skoko, K. Furić, A. Gajović, Mater. Lett. 57 (2003) 4509.
[45] A. Erdőhelyi, K. Fodor, G. Suru, Appl. Catal. A 139 (1996) 131.
[46] Y. Sato, Y. Soma, T. Miyao, S. Naito, Appl. Catal. A 304 (2006) 78.